Volume 269, number 2, 297-304 FEBS 08771 September 1990

An analysis of pseudocontact shifts and their relationship to structural features of the redox states of cytochrome b_5

Nigel C. Veitch[1], David Whitford[2] and Robert J.P. Williams[1]

[1]*Inorganic Chemistry Laboratory and* [2]*Department of Biochemistry, University of Oxford, South Parks Road, Oxford, OX1 3QR, UK*

Received 11 June 1990

The assignment of proton resonances in both redox states of a heme protein is necessary for the evaluation of pseudocontact shift data. Many new assignments are presented here for cytochrome b_5, particularly in the paramagnetic oxidised state, thereby allowing both the calculation of electronic g-tensor values with the magnetic axis orientation and a comparison of observed and calculated pseudocontact shifts utilising a computational procedure. The possible redox linked conformational changes are found to be minimal in contrast with cytochrome c although the procedure additionally highlights aspects of the mobility of certain residues in cytochrome b_5. In this respect the residue Gly-42 appears mobile both by this method and by the observation from NMR spectra of a major and minor conformation in this region.

Cytochrome b_5; Pseudocontact shift; Protein conformation; Nuclear magnetic resonance; Cytochrome c

1. INTRODUCTION

The use of paramagnetic shift data derived from NMR studies of heme proteins is a potentially powerful method for comparative analysis of the structures of the proteins in diamagnetic Fe(II) and paramagnetic Fe(III) redox states. An ideal system for this method of analysis is the electron transfer protein cytochrome b_5 in the form of a heme binding fragment of 82 amino acid residues released from the microsomal membrane by tryptic solubilization [1,2]. However, proton resonance assignments made to date for the paramagnetic oxidised state of cytochrome b_5 [3-6] are not sufficient for detailed comparisons although an extensive set is available for the diagmagnetic reduced state [7]. Here the assignments for the oxidised state are significantly extended to provide approximately 260 proton resonances to facilitate the pseudocontact shift analysis.

The paramagnetic contribution to the observed chemical shift can be classified using the expression:

$$\delta_{para} = \delta_{con} + \delta_{pc}$$

where δ_{con} and δ_{pc} represent the contact (scalar) and pseudocontact (dipolar) terms respectively [8]. While the former influences the shifts of protons on groups directly bonded to the iron atom, such as those of the heme and axial ligands, the pseudocontact term dominates shifts for amino acid residue protons of the polypeptide chain. For an iron (III) low spin heme such as the oxidised state of cytochrome b_5, the pseudocontact shift, expressed in terms of electronic g-tensor values, is defined as:

$$\delta_{pc} = \frac{-N\beta^2 S(S+1)}{9kT}\left\{\left[g_z^2 - \tfrac{1}{2}(g_x^2+g_y^2)\frac{(3\cos^2\theta - 1)}{r^3}\right] + \tfrac{3}{2}\left[(g_x^2 - g_y^2)\frac{(\sin^2\theta \cos 2\varphi)}{r^3}\right]\right\}$$

where g_x,g_y and g_z are the principal values of the g-tensor defining the magnetic axes in a polar coordinate system (r,θ,φ) which describes atomic positions with respect to the central iron atom of the heme [9] and β is the Bohr magneton, S, the electron spin quantum number, N, Avogadro's number and T, absolute temperature. Using a set of experimentally measured redox state shifts δ_{obs}, where $\delta_{obs} = \delta_{ox} - \delta_{red}$ and δ_{ox} and δ_{red} represent the chemical shifts in oxidised and reduced states respectively, the theoretical pseudocontact shifts can be calculated using a computational procedure and coordinates derived from an X-ray crystal structure. Significant differences between observed and calculated pseudocontact shifts can then be related to either structural differences between crystal and solution states or to possible redox linked conformational changes. The viability of such a procedure was originally established with cytochrome c using a limited number of resonance assignments [10] and also illustrated in recent analyses both of the heme pocket of cyanometmyoglobin [11] and again of cytochrome c [12], taking advantage in the latter case of the large number of proton assignments now available in both oxidised and

Correspondence address: N.C. Veitch, Inorganic Chemistry Laboratory, University of Oxford, South Parks Road, Oxford OX1 3QR, UK

Published by Elsevier Science Publishers B.V. (Biomedical Division)
00145793/90/$3.50

Table I

Proton resonance assignments for cytochrome b_5 with observed and calculated pseudocontact shifts

		δ_{ox}	δ_{red}[e]	δ_{pc}	
				obs.	calc.
Val-4	HA	3.77	3.82	−0.05	−0.04
	HB	1.54	1.57	−0.03	−0.03
	HG1	0.29	0.34	−0.05	−0.05
	HG2	0.61	0.65	−0.04	−0.03
Lys-5	HN	8.05	8.11	−0.06	−0.06
	HA	4.04	4.08	−0.04	−0.05
Tyr-6	HN	8.11	8.17	−0.06	−0.06
	HA	5.63	5.71	−0.08	−0.08
	HB1	2.59	2.65	−0.06	−0.06
	HB2	2.77	2.85	−0.08	−0.07
	HD	6.81[b]	6.84	−0.03	−0.06
	HE	6.52[b]	6.55	−0.03	−0.04
Tyr-7	HN	8.64	8.75	−0.09	−0.10
	HA	5.09	5.17	−0.08	−0.10
	HB1	2.37	2.52	−0.15	−0.14
	HB2	3.11	3.23	−0.12	−0.14
	HD	6.84[b]	6.94	−0.10	−0.12
	HE	6.48[b]	6.57	−0.09	−0.11
Thr-8	HN	9.15	9.23	−0.08	−0.10
	HA	4.53	4.64	−0.11	−0.10
	HB	4.82	4.88	−0.06	−0.08
	HG	1.18	1.22	−0.04	−0.07
Leu-9	HN	9.52	9.60	−0.08	−0.11
	HA	3.95	4.08	−0.13	−0.16
	HB1	1.51	1.62	−0.11	−0.13
	HB2	1.67	1.77	−0.10	−0.12
Glu-10	HN	8.38	8.46	−0.08	−0.10
	HA	3.87	3.96	−0.09	−0.10
	HB1	1.89	1.96	−0.07	−0.08
	HB2	1.98	2.05	−0.07	−0.08
Glu-11	HN	7.62	7.71	−0.09	−0.10
	HA	4.03	4.10	−0.07	−0.09
	HB1	2.26	2.32	−0.06	−0.08
	HB2	2.39	2.46	−0.07	−0.10
Ile-12	HN	8.42	8.57	−0.15	−0.14
	HA	3.53	3.72	−0.19	−0.17
	HB	1.78	1.98	−0.20	−0.20
	HG2	0.66	0.94	−0.28	−0.27
Glu-13	HN	8.17	8.33	−0.16	−0.15
	HA	4.27	4.42	−0.15	−0.19
Lys-14	HN	7.11	7.23	−0.12	−0.12
	HA	3.96	4.03	−0.07	−0.09
	HB1	1.40	1.46	−0.06	−0.09
	HB2	1.55	1.59	−0.04	−0.07
His-15	HN	7.74	7.89	−0.15	−0.14
	HA	4.04	4.10	−0.06	−0.09
	HD2	6.83[b]	6.96	−0.13	−0.08
	HE1	7.86[b]	7.95	−0.09	−0.09
Asn-16	HN	7.26	7.34	−0.08	−0.08

(continued)

Table I (*continued*)

		δ_{ox}	δ_{red}[e]	δ_{pc}	
				obs.	calc.
Asn-17	HN	8.00	8.06	−0.06	−0.05
	HA	5.01	4.96	0.05	0.01
	HB1	2.74	2.72	0.02	0.05
	HB2	3.11	3.09	0.02	0.01
Lys-19	HN	7.87	7.82	0.05	0.05
	HA	4.24	4.14	0.10	0.06
Ser-20	HN	7.24	7.20	0.04	0.02
	HA	4.89	4.86	0.03	0.00
	HB1	3.52	3.52	0.00	−0.06
	HB2	3.82	3.82	0.00	−0.04
Thr-21	HN	8.94[d]	8.92	0.02	−0.02
	HA	4.40[d]	4.47	−0.07	−0.13
	HB	3.64	3.57	−0.07	−0.01
	HG	0.80	0.92	−0.12	−0.16
Trp-22	HN	8.76	8.95	−0.19	−0.24
	HA	6.16	6.51	−0.35	−0.38
	HB1	2.93	3.21	−0.28	−0.26
	HB2	2.68	3.02	−0.34	−0.32
	HD1	6.80	6.94	−0.14	−0.18
	HE1	8.66	8.73	−0.07	−0.11
	HE3	6.52[b]	6.70	−0.18	−0.20
	HH3	6.31[b]	6.38	−0.07	−0.10
	HZ3	5.68[b]	5.80	−0.12	−0.14
	HZ2	6.62[b]	6.69	−0.07	−0.10
Leu-23	HN	8.38	8.98	−0.60	−0.58
	HA	4.43	5.03	−0.60	−0.63
	HG	0.70	1.72	−1.02	−1.18
	HD1	−0.61[c]	1.03	−1.64	−1.65
	HD2	−0.75[c]	1.08	−1.83	−2.11
Ile-24	HN	8.03	8.65	−0.62	−0.69
	HA	4.98	5.52	−0.54	−0.53
	HB	1.24	1.70	−0.46	−0.43
	HG2	0.59	0.90	−0.31	−0.32
Leu-25	HN	8.36	8.85	−0.49	−0.45
	HA	4.36	4.91	−0.55	−0.49
	HB1	1.26	1.88	−0.62	−0.50
	HB2	0.10	0.60	−0.50	−0.35
	HG	−0.16	1.07	−1.23	−1.23
	HD1	−0.84[c]	0.64	−1.48	−1.48
	HD2	−2.10[c]	−0.48	−1.62	−1.52
His-26	HN	9.20	9.47	−0.27	−0.17
	HA	3.75	3.83	−0.08	−0.06
	HD2	7.03[b]	7.02	0.01	0.26
	HE1	8.25[b]	8.34	−0.09	0.36
Tyr-27	HN	8.21	8.38	−0.17	−0.16
	HA	3.70	3.87	−0.17	−0.15
	HD	7.01	7.10	−0.09	−0.07
	HE	6.93	6.99	−0.06	−0.05
Lys-28	HN	8.22	8.46	−0.24	−0.18
	HA	4.66	4.88	−0.22	−0.16

(continued)

Table I (*continued*)

		δ_{ox}	δ_{red}[e]	δ_{pc}	
				obs.	calc.
Val-29	HN	8.27	8.48	−0.21	−0.21
	HA	4.04	4.45	−0.41	−0.37
	HB	1.00	1.20	−0.20	−0.22
	HG1	0.01	0.29	−0.28	−0.27
	HG2	0.54	0.77	−0.23	−0.21
Tyr-30	HN	8.81	9.34	−0.53	−0.51
	HA	4.38	4.79	−0.41	−0.36
	HD	6.56[b]	7.27	−0.71	−0.58
	HE	6.42[b]	6.88	−0.46	−0.36
Asp-31	HN	8.11	8.37	−0.26	−0.28
	HA	4.97	5.24	−0.27	−0.24
Leu-32	HN	8.34	8.53	−0.19	−0.30
	HA	4.25	4.30	−0.05	−0.13
	HG	0.92	1.60	−0.68	−0.81
	HD1	−0.59[c]	0.89	−1.48	−1.50
	HD2	−0.12[c]	0.58	−0.70	−0.72
Thr-33	HN	8.66	8.64	0.02	−0.03
	HA	3.70	3.49	0.21	0.16
	HB	4.32	4.24	0.08	0.04
	HG	1.38	1.24	0.14	0.11
Lys-34	HN	8.83[d]	8.67	0.16	0.11
Phe-35	HN	8.11	7.68	0.43	0.32
	HA	5.14	4.41	0.73	0.59
	HB1	2.88	2.44	0.44	0.25
	HB2	2.54	1.93	0.61	0.44
	HD	7.56	6.58	0.98	0.61
	HE	8.40	6.52	1.88	1.34
	HZ	7.67	7.20	0.47	0.68
Leu-36	HN	7.82	7.05	0.77	0.66
	HA	4.82	2.93	1.89	1.57
	HB1	2.38	1.54	0.84	0.65
	HB2	2.10	1.02	1.08	0.88
	HG	2.49	1.72	0.77	0.76
	HD1	1.22	0.46	0.76	0.67
	HD2	1.30	0.77	0.53	0.38
Glu-37	HN	8.54	7.57	0.97	0.83
	HA	4.91	3.75	1.16	1.16
Glu-38	HN	8.26	7.02	1.24	1.28
	HA	4.86	3.97	0.89	0.81
His-39	HN	8.87	6.05	2.82	2.65
Gly-42	HN	10.43	6.14	4.29	6.41
	HA1	6.05	3.92	2.13	2.43
	HA2	5.72	3.34	2.38	2.63
Glu-43	HN	9.97	8.13	1.84	1.76
	HA	5.83	3.53	2.30	2.44
Glu-44	HN	9.56	8.26	1.30	1.17
	HA	4.23	3.66	0.57	0.57

(*continued*)

Table I (*continued*)

		δ_{ox}	δ_{red}[e]	δ_{pc}	
				obs.	calc.
Val-45	HN	9.29[d]	8.22	1.07	1.29
	HA	4.06[d]	4.04	0.02	−0.07
	HB	2.21	2.56	−0.35	0.63
	HG1	1.47	0.77	0.70	2.24
	HG2	1.58[a]	0.97	0.61	−0.97
Leu-46	HN	7.29	5.97	1.32	1.15
	HA	3.09	3.85	−0.76	−1.18
Arg-47	HN	8.42	8.05	0.37	0.44
Glu-48	HN	8.10	8.07	0.03	−0.10
	HA	3.96	4.06	−0.10	−0.16
Gln-49	HN	6.58	7.08	−0.50	−0.61
	HA	4.13	4.57	−0.44	−0.59
Ala-50	HN	6.84[d]	7.23	−0.39	−0.42
	HA	3.74[d]	4.17	−0.43	−0.52
Gly-51	HN	9.33	9.75	−0.42	−0.39
	HA1	3.89	4.09	−0.20	−0.25
	HA2	3.53	3.77	−0.24	−0.27
Gly-52	HN	7.37	7.79	−0.42	−0.48
	HA1	3.52	3.86	−0.34	−0.40
	HA2	4.22	4.53	−0.31	−0.34
Asp-53	HN	8.22	8.50	−0.28	−0.38
Ala-54	HN	8.16	9.03	−0.87	−0.74
	HA	4.39	5.20	−0.81	−1.04
	HB	0.11[c]	1.76	−1.65	−1.85
Thr-55	HN	8.04	8.61	−0.57	−0.58
	HA	2.85	3.30	−0.45	−0.25
	HB	3.78	3.97	−0.19	−0.11
	HG	0.37	0.39	−0.02	0.10
Glu-56	HN	8.43	8.69	−0.26	−0.22
	HA	3.92	3.82	0.10	0.11
Asn-57	HN	7.62	7.97	−0.35	−0.54
	HA	4.26	4.46	−0.20	−0.46
Phe-58	HN	7.98	8.69	−0.71	−0.70
Glu-59	HN	8.76	8.26	0.50	0.83
	HA	5.41	3.76	1.65	2.16
Asp-60	HN	8.84	8.08	0.76	0.76
	HA	4.83	4.19	0.64	0.67
	HB1	2.98	2.75	0.23	0.26
	HB2	2.82	2.54	0.28	0.27
Val-61	HN	8.12	6.63	1.49	1.83
	HA	4.40	3.18	1.22	0.83
Gly-62	HN	8.93	6.49	2.44	1.66
	HA1	4.88	3.37	1.51	1.34
	HA2	5.09	3.16	1.93	1.92

(*continued*)

Table I (*continued*)

		δ_{ox}	δ_{red}[e]	δ_{pc}	
				obs.	calc.
His-63	HN	11.13	6.23	4.90	5.49
	HA	7.37[a]	2.57	4.80	5.60
	HB1	9.87[a]	0.37	9.50	8.57
	HB2	10.07[a]	1.07	9.00	8.66
Ser-64	HN	11.67	9.74	1.93	1.37
	HA	4.95	4.03	0.92	1.06
Thr-65	HN	9.26	8.73	0.53	0.46
	HA	4.47	3.77	0.70	0.60
Asp-66	HN	8.27	8.01	0.26	0.14
Ala-67	HN	8.83[d]	8.57	0.26	0.32
	HA	4.10[d]	4.65	−0.55	−0.57
	HB	2.45	1.21	1.24	1.96
Arg-68	HN	9.22	8.13	1.09	1.03
	HA	4.46	3.53	0.93	0.94
Glu-69	HN	9.02	8.67	0.35	0.28
	HA	4.25	4.12	0.13	0.10
Leu-70	HN	8.33	8.35	−0.02	−0.10
	HA	4.19	4.35	−0.16	−0.22
	HB1	1.73	2.05	−0.33	−0.49
	HB2	2.06	2.66	−0.60	−0.55
	HG	1.41	1.84	−0.43	−0.51
Ser-71	HN	8.42	8.75	−0.33	−0.10
	HA	3.86	4.11	−0.25	−0.48
Lys-72	HN	7.19[d]	7.28	−0.09	−0.10
	HA	4.04	4.18	−0.14	−0.12
Thr-73	HN	7.63	7.87	−0.24	−0.17
	HA	3.95	4.01	−0.06	−0.10
	HB	3.68	3.77	−0.09	−0.16
	HG	0.99	1.10	−0.11	−0.07
Phe-74	HN	7.24	7.60	−0.36	−0.22
	HA	4.79	5.00	−0.21	−0.16
	HD	7.00[b]	7.29	−0.29	−0.27
	HE	6.75[b]	6.85	−0.10	−0.09
	HZ	7.12[b]	7.03	0.09	0.06
Ile-75	HN	6.80	6.98	−0.18	−0.18
	HA	3.45	3.70	−0.25	−0.25
	HB	1.42	1.55	−0.13	−0.17
	HG2	0.72	0.86	−0.14	−0.11
Ile-76	HN	8.59	8.85	−0.26	−0.20
	HA	4.52	4.65	−0.13	−0.12
	HB	1.76	1.84	−0.08	−0.12
	HG11	0.16[c]	0.31	−0.15	−0.21
	HG12	−0.11[c]	0.09	−0.19	−0.17
	HG2	0.67	0.80	−0.13	−0.13
	HD	−1.20[c]	−1.06	−0.14	−0.16
Gly-77	HN	7.29	7.48	−0.19	−0.15
	HA1	3.99	4.12	−0.13	−0.11
	HA2	4.33	4.46	−0.13	−0.09
Glu-78	HN	8.96	9.09	−0.13	−0.10
	HA	5.17[d]	5.32	−0.15	−0.13
Leu-79	HN	8.84	8.99	−0.15	−0.13
	HA	4.59	4.75	−0.16	−0.13
	HG	1.82	1.93	−0.11	−0.12
His-80	HN	9.02	9.12	−0.10	−0.10
	HA	3.72	3.78	−0.06	−0.07
	HB1	2.52	2.60	−0.08	−0.08
	HB2	2.89	6.97	−0.08	−0.08
	HD2	6.90[b]	6.98	−0.08	−0.06
	HE1	7.52[b]	7.57	−0.05	−0.04
Pro-81	HA	3.61	3.64	−0.03	−0.05
Asp-82	HN	11.06	11.12	−0.06	−0.05
	HA	4.43	4.46	−0.03	−0.05
	HB1	2.59	2.62	−0.03	−0.05
	HB2	2.67	2.71	−0.04	−0.05
Asp-83	HN	8.16	8.26	−0.10	−0.07
	HA	4.93[d]	5.00	−0.07	−0.08
	HB1	2.58	2.66	−0.08	−0.09
	HB2	3.06	3.13	−0.07	−0.11
Arg-84	HN	6.99	7.03	−0.04	−0.07
	HA	4.03	4.08	−0.05	−0.09

Resonance assignments are for the bovine tryptic fragment of cytochrome b_5 at 30°C in 20 mM potassium phosphate, pH 7.0. Chemical shift values are referred to 1,4-dioxan, with a resonance at 3.74 ppm relative to 2,2-trimethyl-2-silapentane-5-sulphonate and are quoted to ±0.02 ppm. $AF_{axial} = 5.25$, $AF_{rhombic} = -2.31$, $\Sigma(\delta_{calc}-\delta_{obs})^2 = 5.9$ (omitting sidechains of Phe and Tyr residues, H26 HD2 & HE1, G42 HN, V45 HB, HG1 & HG2). [a] In agreement with [4]. [b] In agreement with [5]. [c] In agreement with [6]. [d] Corrected from [3]. [e] In agreement with [7], given the temperature difference between the two sets of assignments.

reduced protein states [13,14]. It is clear that subtle structural differences can be detected and furthermore that the method is useful in resolving ambiguity in assignments and giving stereospecific assignments.

2. MATERIALS AND METHODS

Protein preparation and NMR measurements were as previously described [3].

2.1. *Computational procedures*

Theoretical pseudocontact shifts were calculated using the FORTRAN program DISMET in conjunction with the X-ray crystallographic coordinates to define proton positions. The program optimises g-tensor values in terms of axial and rhombic anisotropy factors defined as:

$$AF_{axial} = g_z^2 - \tfrac{1}{2}(g_x^2 + g_y^2)$$

$$AF_{rhombic} = (g_x^2 - g_y^2)$$

in conjunction with the Eulerian rotation angles (α,β,γ) defining the orientation of the magnetic axes [10]. The best fit of calculated and observed shifts was assessed by a least squares analysis procedure. Calculations were performed both with the complete data set given in Table I and with a slightly smaller set with certain residues omitted for reasons given below.

3. RESULTS

3.1. *Proton resonance assignments*

The assignments presented for ferricytochrome b_5 were obtained using sequential assignment techniques [15] and were made with reference to previously published data on this redox state [3–6], as summarised in Table I. However, although the data on ferricytochrome b_5 are considerably extended, sequential assignment procedures were limited by difficulties encountered when working in H_2O solutions through the presence of a broad labile proton resonance downfield of the solvent resonance, a feature absent from D_2O solutions. This feature, whose origin remains unclear, may arise from water molecules in the vicinity of the heme iron which cannot exchange rapidly with bulk solvent molecules and thus experience paramagnetic broadening. Sequential assignments as shown in Fig. 1 were in agreement with the pattern of backbone proton connectivities observed in the complete sequence specific assignment of ferrocytochrome b_5 [7]. These data were collected at 40°C whereas the data on this redox state presented in Table I were obtained independently at 30°C.

In the amide region of NOESY spectra of ferricytochrome b_5 it was further noted that two separate sets of NOE connectivities involving the residue Gly-42 existed, as shown in Fig. 2. The second set, of weaker intensity and with proton chemical shifts to slightly lower field can be followed from Gly-42 through to Glu-44. The Gly-42 HA1–HA2 crosspeaks are again seen in COSY spectra with differing intensity. The two sets of signals observed indicate an additional minor conformation in this region principally involving the residue

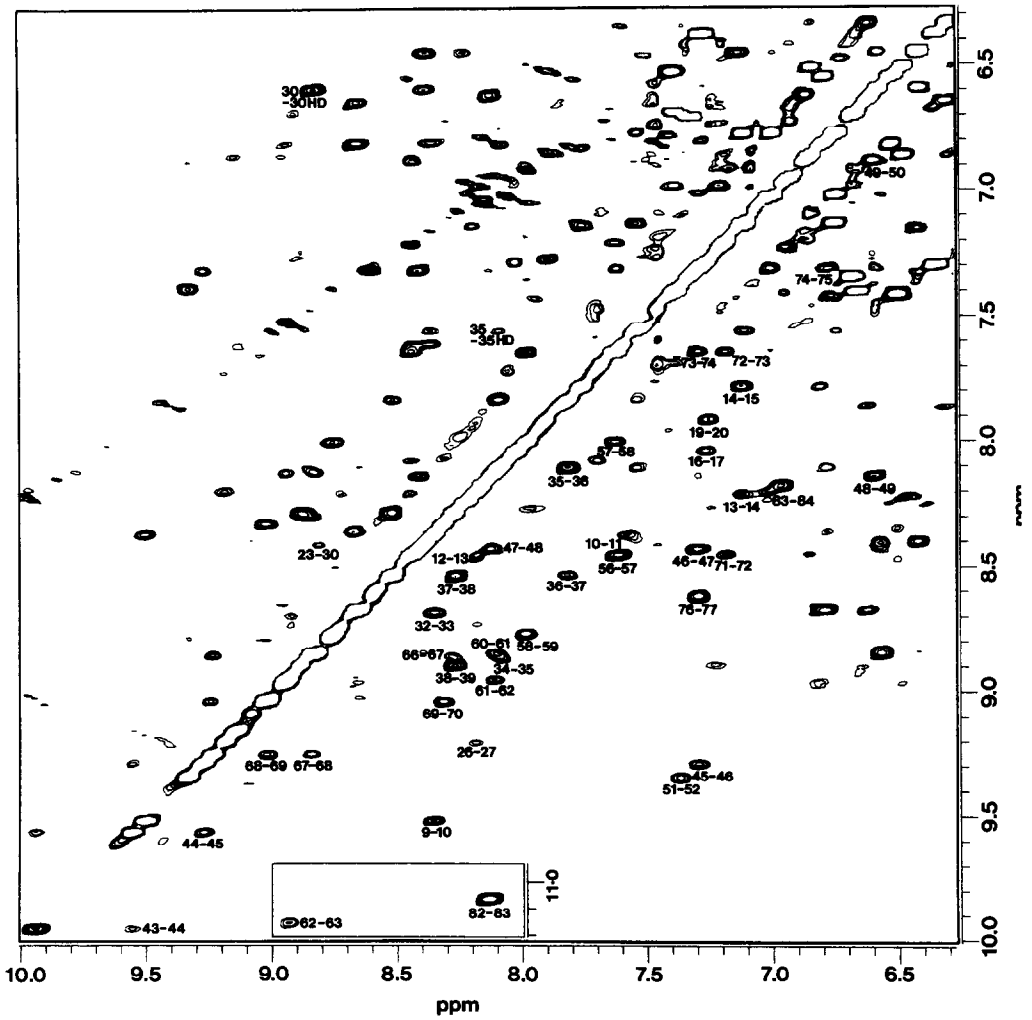

Fig. 1. Phase-sensitive 500 MHz NOESY spectrum of ferricytochrome b_5 illustrating NOE connectivities between sequential backbone amide protons (below diagonal) and between amide and aromatic protons (above diagonal). The spectrum was recorded in 90% H_2O:10% D_2O with 20 mM potassium phosphate at pH 7.0, 30°C and with a protein concentration of 5 mM. The mixing time employed was 135 ms.

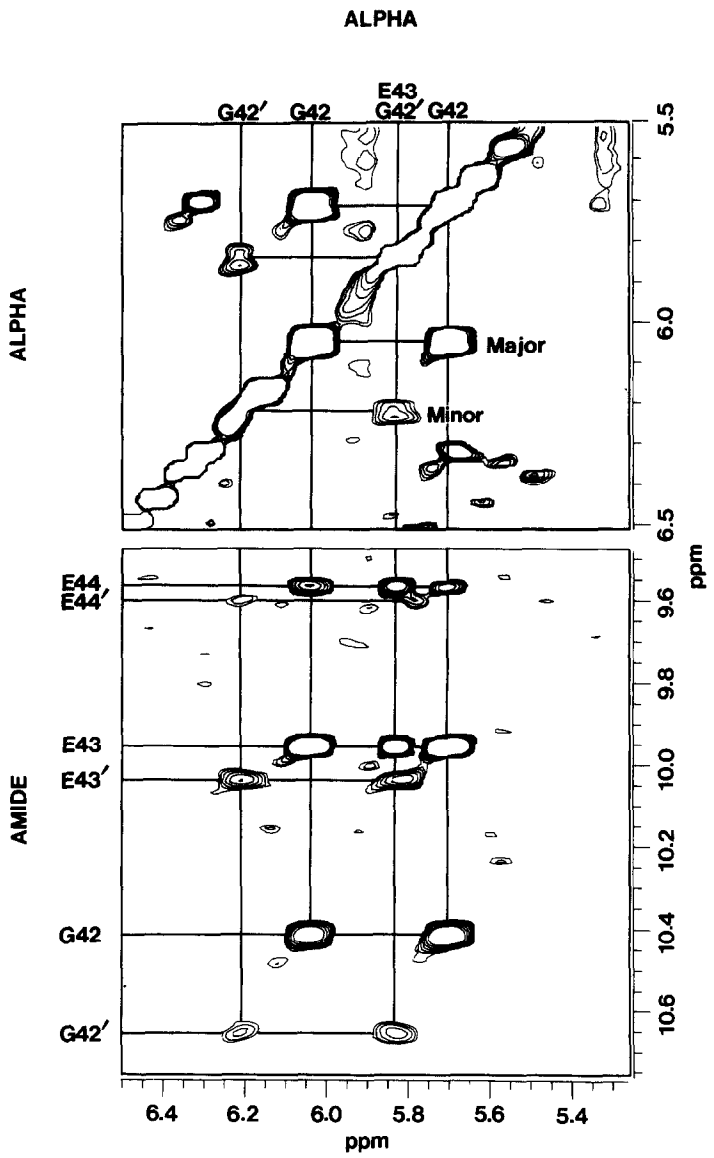

Fig. 2. Sequential backbone NOE connectivities from Gly-42 to Glu-44 in the α and amide proton regions from the phase sensitive 500 MHz NOESY spectrum of ferricytochrome b_5. Cross peaks arising from a minor conformation for these residues are indicated by an assignment marked with a dash. The spectrum was recorded in 90% H_2O:10% D_2O with 20 mM potassium phosphate at pH 7.0, 30°C and a protein concentration of 5 mM. The mixing time employed was 135 ms.

Gly-42. It was not possible to assess whether the same feature occurred in ferrocytochrome b_5 as the dispersion of the amide signals was not sufficient to identify possible major and minor forms.

Stereospecific assignments were made for valine and leucine methyl protons from NOE connectivities in NOESY spectra and correlation with expected near neighbour distances derived from the crystal structure. One of the methyl groups typically shows a strong intraresidue NOE to its HA proton.

3.2. *Calculation of g-values and Eulerian angles*

The overall correlation between calculated and observed pseudocontact shifts was found to be excellent following optimisation of g-values and Eulerian angles and is reflected in a total for the summed squares of differences of only 5.90 when clearly understood anomalous values (see Discussion) are omitted from the data set. Values obtained for the axial and rhombic anisotropy factors were close to those calculated from the g-values $g_x = 1.43$, $g_y = 2.23$, $g_z = 3.03$ measured by ESR in a frozen solution at 77K [16]. The fit between calculated and observed pseudocontact shifts did not vary greatly with the magnitude of the anisotropy factors but was heavily dependent on the orientation of the magnetic axes expressed by the Eulerian angles, in parallel with the situation found for cytochrome c [10,12]. The optimised Eulerian angles were $\alpha = -15°$,

$B = -7°$ and $\gamma = 83°$ which are similar to the proposals of an earlier study based on a small number of redox state shifts [17].

Several stereospecific assignments were confirmed by the excellent fit between calculated and observed pseudocontact shifts for the pairs of methyl groups. Although a small number of HB protons were assigned in a similar manner to methyl groups, the remainder together with the HA protons of Gly residues were assigned on the basis of the best fit to the pseudocontact shift data.

4. DISCUSSION

Comparison of the individual calculated and observed pseudocontact shifts indicates that there are effectively no significant differences for the backbone protons and that only a small number of sidechains from the complete data set presented in Table I exhibit a poor fit. The immediate conclusions are that structural differences between (i) the solution and the crystal states and (ii) the oxidised and reduced forms of the protein are few.

The behaviour of the exceptional resonances showing poor agreement can, however, be interpreted in terms of the mobility of residues as compared with the static picture provided from the X-ray coordinates [18,19]. The distribution of these residues is indicated on a schematic representation of the cytochrome b_5 fold shown in Fig. 3 [20]. An illustration of mobility is seen with the aromatic sidechains of phenylalanine and tyrosine residues which from NMR data are known to be rapidly flipping. The pseudocontact shift calculation based on fixed proton positions cannot match those observed although it is noted that the average of the calculated shift for the pairs of protons HD1/HD2 and HE1/HE2 falls close to the experimental value with the exception of Phe-35. This sidechain is close to the heme group and a relatively minor orientational change would significantly affect the pseudocontact term. Other sidechains close to the heme, such as that of Ala-67, also fall into this category. In general the calculated and observed pseudocontact shifts for all of the valine and leucine sidechains correlate well, with the notable exception of Val-45. While the HN and HA protons of this residue show an excellent fit, the correlation for HB and methyl protons is poor. This is postulated to arise by virtue of the mobility of this sidechain which must be rapidly reorienting about the CA-CB bond. In support of this, it is seen that the HG1 and HG2 chemical shifts are very similar in both oxidation states. A calculated average chemical shift for the oxidised HG1 and HG2 methyl resonances was found to be close to 1.5 ppm. The behaviour of this valine sidechain appears to be unique in cytochrome b_5 but is parallel by the residue Val E11 in metmyoglobin [11]. Another significant difference in this region of the fold

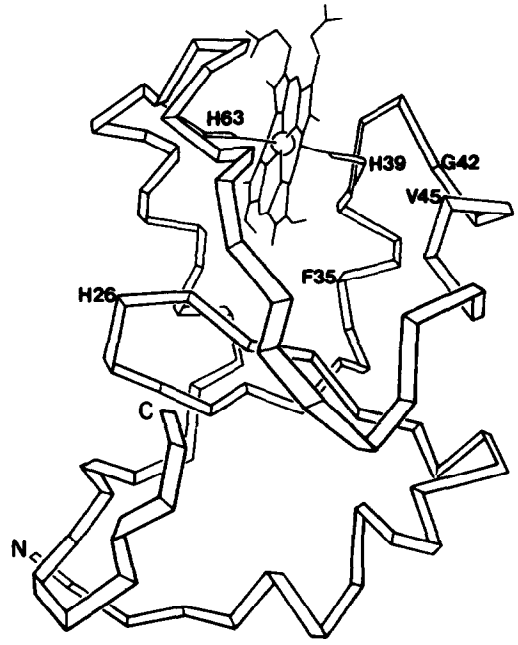

Fig. 3. Schematic ribbon diagram of the cytochrome b_5 heme binding fragment after Mathews [20], illustrating the location of amino acid residues with protons that show a relatively poor fit between observed and calculated pseudocontact shifts. The two heme ligating histidine residues, His-39 and His-63, are also indicated.

occurs with the HN shift of Gly-42 although the HA protons of this residue fit well. The sequence in this region from the axial heme ligand His-39 runs His-Pro-Gly-Gly-Glu-Glu-Val and has been classified as a β-bend leading into α-helix III beginning at Glu-43 [18]. The second Gly residue appears to be conformationally mobile as is also confirmed by the observation of two sets of proton resonances indicating a major and minor form of Gly-42 in solution. This local feature does not appear to be related to the two forms of cytochrome b_5 noted previously which differ in the orientation of the heme group [6,21]. These isomers, occurring in an 8:1 equilibrium ratio, were found to result from a 180° rotation of the heme about the α,γ-meso proton axis. Some small differences in amino acid side chain orientation were suggested between the two forms for residues in the heme pocket [21]. It seems unlikely that this heme disorder could account for the distinct differences seen in the Gly-42 region as this is more distant from the immediate heme environment and also corresponding effects which might be expected for other similarly located residues have not been noted. Mobility of a Gly-Gly sequence has been suggested before in analyses of NMR spectra of yeast iso-1-cytochrome c where it has proved impossible to assign the sequence of two glycines at positions 83 and 84 [22].

An unusual discrepancy is noted for the aromatic protons of His-26, a residue lying on the surface of the protein [18]. Although the observed pseudocontact shifts are close to zero, those calculated have a signifi-

cant value and in the case of the HE1 proton are of opposite sign. Diffraction studies show that His-26 is not involved in hydrogen bonding but is instead associated with the carboxyl protons of Glu-59 in an electrostatic interaction [18]. In the NOESY spectra of both oxidised and reduced forms, strong NOE connectivities are seen from His-26 HE1 to Glu-59 HG1, HG2 (at 3.02 and 3.13 ppm) and Thr-55 HG as expected from the crystal structure. Thus there is no apparent difference between solution and crystal states which might explain this anomaly. In view of the above discrepancy and the observation that His-26, with a pK_a of 6.9 [23], must exist in both protonated and deprotonated forms at the pH of our study, it is likely therefore that the NMR paramagnetic shift for this residue is some average of different structures which cannot be reconciled easily with the crystal structure data. There is always a danger in NOE data in that certain states are over-represented.

In conclusion, this study has demonstrated the use of the pseudocontact shift for a comparative study of the solution structure of cytochrome b_5 in both oxidised and reduced states. The shift data extend to 29 Å from the heme iron atom with subsequent analysis showing that the redox switch between oxidised and reduced cytochrome b_5 generates no noticeable conformational change in solution, a feature which contrasts with the case for cytochrome *c* [12]. This observation agrees with crystal studies showing that cytochrome b_5 but not cytochrome *c* can be reduced in the crystal without break-up [18,24,25]. Furthermore, the method allows details of local mobility to be characterised which are not observed from diffraction studies.

Acknowledgements: The authors would like to thank Dr. David Concar and Yuan Gao for their assistance with the computation and Dr. Jonathan Boyd and Nick Soffe for advice concerning NMR experiments. This study was supported by the Science and Engineering Research Council (R.J.P.W) and the Nuffield Foundation (D.W.). N.C.V. thanks Merton College, Oxford for the provision of a Harmsworth Senior Scholarship. R.J.P.W. is a member of the Oxford Centre for Molecular Sciences.

REFERENCES

[1] Reid, L.S. and Mauk, A.G. (1982) J. Am. Chem. Soc. 104, 841–845.
[2] Strittmatter, P. (1967) Methods Enzymol. 10, 553–556.
[3] Veitch, N.C., Concar, D.W., Williams, R.J.P. and Whitford, D. (1988) FEBS Lett. 238, 49–55.
[4] McLachlan, S.J., La Mar, G.N. and Lee, K.-B. (1988) Biochim. Biophys. Acta 957, 430–455.
[5] Reid, L.S., Gray, H.B., Dalvit, C., Wright, P.E. and Saltmann, P. (1987) Biochemistry 26, 7102–7107.
[6] Keller, R.M. and Wüthrich, K. (1980) Biochim. Biophys. Acta 621, 204–217.
[7] Guiles, R.D., Altman, J., Kuntz, I.D. and Waskell, L. (1990) Biochemistry 29, 1276–1289.
[8] Jardetzky, O. and Roberts, G.C.K. (1981) in: NMR in Molecular Biology, Academic Press, New York, pp. 69–83.
[9] Kurland, R.J. and McGarvey, B.R.J. (1970) J. Magn. Reson. 2, 289–301.
[10] Williams, G., Clayden, N.J., Moore, G.R. and Williams, R.J.P. (1985) J. Mol. Biol. 183, 447–460.
[11] Emerson, S.D. and La Mar, G.N. (1990) Biochemistry 29, 1556–1566.
[12] Feng, Y., Roder, H. and Englander, S.W. (1990) Biochemistry 29, 3494–3504.
[13] Wand, A.J., Di Stefano, D.L., Feng, Y., Roder, H. and Englander, S.W. (1989) Biochemistry 28, 186–194.
[14] Feng, Y., Roder, H., Englander, S.W., Wand, A.J. and Di Stefano, D.L. (1989) Biochemistry 28, 195–203.
[15] Wüthrich, K. (1986) in: NMR of Proteins and Nucleic Acids, Wiley, New York.
[16] Bois-Poltoratsky, R. and Ehrenberg, A. (1967) Eur. J. Biochem. 2, 361–365.
[17] Keller, R.M. and Wüthrich, K. (1972) Biochim. Biophys. Acta 285, 326–336.
[18] Mathews, F.S., Czerwinski, E.W. and Argos, P. (1979) in: The Porphyrins, vol. VIIB (Dolphin, D. ed.) pp. 107–147, Academic Press, New York.
[19] Argos, P. and Mathews, F.S. (1975) J. Biol. Chem. 250, 747–751.
[20] Mathews, F.S. (1985) Prog. Biophys. Molec. Biol. 45, 1–56.
[21] McLachlan, S.J., La Mar, G.N., Burns, P.D., Smith, K.M. and Langry, K.C. (1986) Biochim. Biophys. Acta 874, 274–284.
[22] Gao, Y., Boyd, J., Williams, R.J.P. and Pielak, G.J. (1990) Biochemistry (in press).
[23] Altman, J., Lipka, J.J., Kuntz, I. and Waskell, L. (1989) Biochemistry 28, 7516–7523.
[24] Takano, T. and Dickerson, R.E. (1981) J. Mol. Biol. 153, 79–94.
[25] Takano, T. and Dickerson, R.E. (1981) J. Mol. Biol. 153, 95–115.